

Tewfik Soulimane,\* Sarah R.  
O'Kane and Olga Kolaj

Department of Chemical and Environmental  
Sciences and Materials and Surface Science  
Institute, University of Limerick, National  
Technology Park, Limerick, Ireland

Correspondence e-mail: tewfik.soulimane@ul.ie

Received 1 December 2009

Accepted 29 January 2010

## Isolation and purification of *Thermus thermophilus* HpaB by a crystallization approach

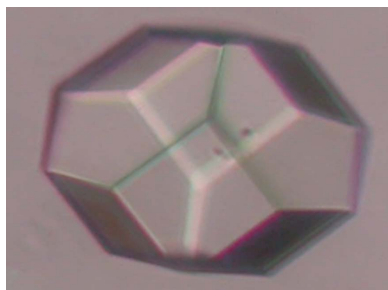
The oxygenase HpaB is a component of the 4-hydroxyphenylacetate 3-mono-oxygenase enzyme that is responsible for the hydroxylation of 4-hydroxyphenylacetate. It utilizes molecular oxygen and a reduced flavin, which is provided by HpaC, the second component of the enzyme. While isolating integral membrane respiratory complexes from *Thermus thermophilus*, micro-crystals of HpaB were formed. Further purification of the enzyme was achieved by repetitive crystallization. Subsequently, well shaped single crystals of the native enzyme that diffract to 1.82 Å resolution were grown in sitting drops. They belong to the orthorhombic space group *I*222, with unit-cell parameters  $a = 91.3$ ,  $b = 99.8$ ,  $c = 131.7$  Å.

### 1. Introduction

Oxygenases play a crucial role in the aerobic catabolic pathway for aromatic compounds by catalyzing its initial steps. Based on their oxygen and cofactor requirements, the complexity of the system and their electron-transfer components, oxygenases can be classified into different categories (Galan *et al.*, 2000). 4-Hydroxyphenylacetate (4HPA) 3-mono-oxygenase is a member of the two-component non-haem flavin-diffusible mono-oxygenase (TC-FDM) family. The hydroxylation of 4HPA by this oxygenase is performed in two stages. Firstly, the reductase component of the enzyme, the small 16.1 kDa protein HpaC, reduces flavin with the use of NAD(P)H. Subsequently, reduced flavin is transported to the oxygenase component (HpaB) of 4HPA 3-mono-oxygenase by free diffusion where, together with the oxygen molecule, it is used for the oxygenation of substrates. While the oxygenase components seem to determine the substrate specificity (Kadiyala & Spain, 1998), it is the reductase component that guarantees the hydroxylation activity of the TC-FDM family members (Cooper & Skinner, 1980; Prieto & Garcia, 1994; Galan *et al.*, 2001; Arias-Barrau *et al.*, 2005; Gibello *et al.*, 1997; Chaïyen *et al.*, 2001; Thotsaporn *et al.*, 2004), despite the lack of physical interaction between the two components (Galan *et al.*, 2000).

Although classified within the same family, the TC-FDM family members exhibit different biophysical and biochemical characteristics. Based on these observations, two groups, with the *Acinetobacter baumannii* and *Escherichia coli* enzymes as representatives, can be identified. The sequence identity of the oxygenase components from *A. baumannii* and *E. coli* ( $C_2$  and HpaB, respectively) is low and the differences between them are also reflected in the flavin specificity for hydroxylation:  $C_2$  uses FADH<sub>2</sub>, FMNH<sub>2</sub> and riboflavin (Sucharitakul *et al.*, 2006), while HpaB reacts either with FADH<sub>2</sub> or FMNH<sub>2</sub> (Xun & Sandvik, 2000). The reductase components of the two enzymes differ significantly in size, with  $C_1$  from *A. baumannii* being almost twice as large as HpaC from *E. coli* (520 and 267 amino acids, respectively). Moreover, unlike its equivalent from *E. coli*,  $C_1$  is stimulated by the presence of the substrate (Sucharitakul *et al.*, 2005).

Recently, the crystal structures of the oxygenase components of representatives of both groups within the TC-FDM family have been solved in ligand-free, flavin-bound and flavin/substrate-bound states. The crystal structure analyses of  $C_2$  from *A. baumannii* (Alfieri *et al.*, 2007) and of an *E. coli*-type HpaB from *Thermus thermophilus* (Kim, Hisano *et al.*, 2007) showed significant differences in the conformational changes introduced upon binding of flavin and substrate, in the



architecture of the active sites and in the substrate-recognition mechanism. Both crystal structures were determined at high resolution using protein produced in *E. coli*-based expression systems. Here, we present a reproducible procedure for the isolation and purification of native HpaB from *T. thermophilus* HB8 using a crystallization approach, leading to structure-grade quality crystals. Moreover, the high-resolution data obtained on a home source suggest the potential for the elucidation of higher resolution structures of native HpaB and of its complex with FAD and 4HPA when the X-ray data are collected at a synchrotron source.

## 2. Materials and methods

### 2.1. Fermentation of *T. thermophilus* HB8

Fermentation of *T. thermophilus* HB8 was performed at the Helmholtz Centre for Infection Research, Braunschweig, Germany. The cells were grown under low oxygen tension ( $0.05 \text{ VV}^{-1} \text{ min}^{-1}$ ; volume air per volume medium and per minute) in culture medium at 343 K in a 100 l fermenter. Cells were harvested at the middle exponential growth phase, yielding approximately 400–500 g biomass.

### 2.2. Isolation of native HpaB using a crystallization approach

HpaB protein was obtained as a side product during the initial purification of *T. thermophilus* respiratory-chain complexes. A detailed purification protocol for isolation of the aforementioned enzymes has been published (Soulimane *et al.*, 2002). 100 g of *T. thermophilus* cells was resuspended in 500 ml 0.25 M Tris–HCl pH 7.6 buffer containing 0.2 M KCl and homogenized. Subsequently, lysozyme was added to a final concentration of  $0.6 \mu\text{M}$  and the suspension was kept under stirring for 3 h at 277 K. After sample centrifugation at 53 936g for 45 min at 277 K, the supernatant containing soluble *T. thermophilus* proteins was discarded and the pellet was resuspended in 500 ml 0.1 M Tris–HCl pH 7.6, homogenized and centrifuged at 53 936g for 30 min at 277 K. In the standard procedure for the purification of *T. thermophilus* respiratory complexes, this washing step was repeated three times in order to further remove the soluble proteins present in the periplasm and the cytoplasm of the *T. thermophilus* cells. For the purpose of purification of HpaB, however, the number of washing steps was decreased to one

(see §3). The washed pellet was subsequently resuspended in 500 ml 0.1 M Tris–HCl pH 7.6 and the suspension was incubated for 3 h at 277 K in the presence of 5% Triton X-100 in order to solubilize the *T. thermophilus* membrane proteins (MPs). After centrifugation at 53 936g for 1 h at 277 K, the resulting supernatant was diluted with water to 5 l and subjected to ion-exchange chromatography using a  $30 \times 10 \text{ cm}$  column packed with DEAE-Biogel agarose (Bio-Rad) equilibrated with 0.01 M Tris–HCl pH 7.6, 0.1% Triton X-100. Elution with 4 l ( $2 \times 2 \text{ l}$ ) of a linear gradient from 0 to 0.25 M NaCl resulted in three distinguished peaks containing, among others, respiratory-chain complexes (Soulimane *et al.*, 2002). Respiratory-chain complexes can be distinguished based on their corresponding reduced–oxidized UV–Vis spectra in the region between 400 and 650 nm. The first peak contained mainly  $ba_3$ -type cytochrome *c* oxidase, the second peak contained  $caa_3$ -type cytochrome *c* oxidase and the third peak was identified to contain succinate dehydrogenase and *bc* complex.

The fractions containing  $caa_3$  cytochrome *c* oxidase (220 ml) were dialyzed against 5 l 0.01 M Tris–HCl pH 7.6, 0.1% Triton X-100. For concentration purposes, the resulting sample was applied onto a TMAE-Fractogel anion-exchange chromatography column (Merck) and eluted in one step using 0.01 M Tris–HCl pH 7.6, 0.05% dodecyl- $\beta$ -D-maltoside (DDM) containing 0.15 M NaCl. This step also served to exchange the harsh detergent Triton X-100 for the mild detergent dodecyl- $\beta$ -D-maltoside (DDM). The resulting  $caa_3$  oxidase fractions ( $\sim 20 \text{ ml}$ ; 28 mg of  $caa_3$  in total) were further concentrated to 2.5 ml using a centrifugal filter (Centricon YM30, Millipore) and applied onto a gel-filtration column (Superdex 200, GE Healthcare). This chromatographic step is used to separate  $caa_3$  cytochrome *c* oxidase fractions from other remaining respiratory complexes such as  $ba_3$  cytochrome oxidase and *bc* complex. After this step the total  $caa_3$  content was  $\sim 19 \text{ mg}$ , while the total protein content in the sample was measured to be 60 mg. The  $caa_3$  oxidase fractions were incubated at 277 K and crystalline HpaB started to form after 15 min (Fig. 1*a*). Following 5 h incubation at 277 K, the supernatant containing the  $caa_3$  oxidase was removed and the crystals were dissolved in 2 ml 0.01 M Tris–HCl pH 7.6 by vortexing for 5 min. Subsequent centrifugation was used to remove precipitated material, which can be seen in Fig. 1*a*). The supernatant, containing 17 mg of protein in total, was incubated at 277 K for a period of 30 min, resulting once again in the formation of crystals of HpaB. This procedure was repeated twice,

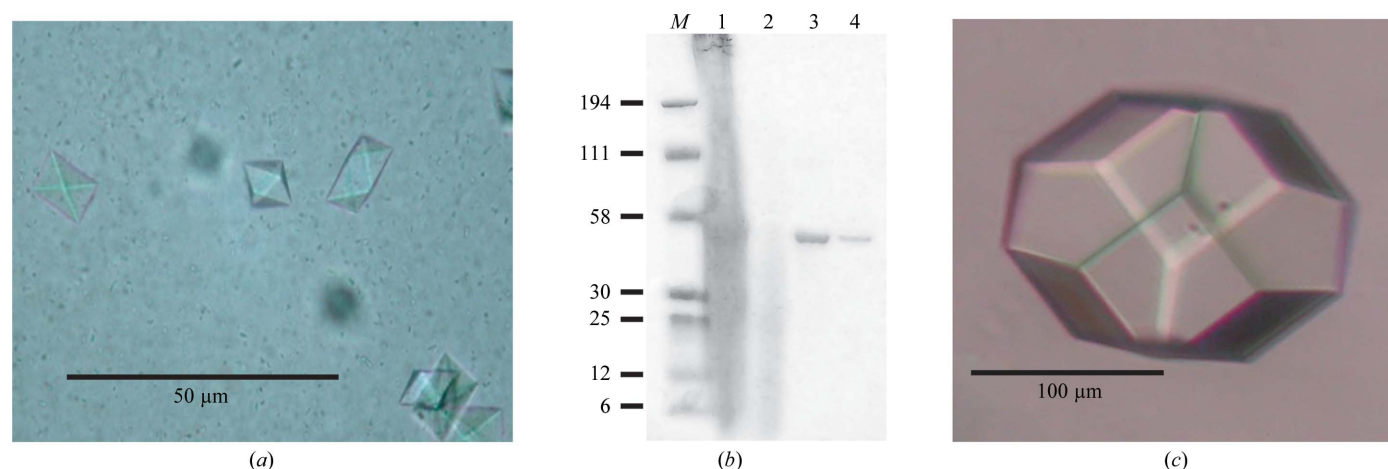


**Figure 1**  
Purification and crystallization of native HpaB from *T. thermophilus*. (a) Spontaneously formed crystals obtained during the purification of membrane proteins from *T. thermophilus* HB8. (b) SDS–PAGE analysis of HpaB purification by crystallization. Lane M, molecular-weight standard markers, with molecular weights shown on the left in kDa; lane 1, HpaB-containing sample of  $caa_3$  after gel filtration on Superdex 200 in which HpaB crystals spontaneously formed; lane 2, supernatant after centrifugation of the crystals (a) that formed in the sample in lane 1; lane 3, dissolved crystals after second purification by crystallization; lane 4, final purified HpaB obtained by dissolving spontaneously formed crystals after the final recrystallization step. (c) Crystals obtained by the sitting-drop vapour-diffusion method under controlled conditions.

dissolving the crystals in 500  $\mu\text{l}$  0.01 *M* Tris–HCl pH 7.6 with a total protein content of 13 and 10 mg, respectively. These values can be accepted as the content of HpaB as at this stage the sample contains almost exclusively the protein of interest (lane 3, Fig. 1*b*). Finally, the resulting crystals were dissolved in 500  $\mu\text{l}$  0.01 *M* Tris–HCl pH 7.6 (lane 4, Fig. 1*b*) and used for crystal growth under controlled conditions as described in §2.4. Overall, 8 mg of highly pure HpaB was obtained using the described procedure. A detailed purification scheme of native HpaB is presented in Fig. 2.

## 2.3. Determination of protein concentration

The total protein concentration was measured using the BCA assay (Smith *et al.*, 1985). The concentration of *caa*<sub>3</sub> oxidase was determined as follows: the haem *a* concentration was measured using the dithionite reduced-minus-oxidized spectrum at 604 nm with an extinction coefficient of 12 000  $M^{-1} \text{ cm}^{-1}$  (van Gelder, 1966). Sub-

sequently, the haem *a* concentration was used to determine the concentration of *caa*<sub>3</sub> oxidase using a haem *a*:protein ratio of 2:1 owing to the presence of two haem *a* molecules within the protein.

## 2.4. Protein crystallization and X-ray investigation

Crystallization of the native HpaB was performed using the sitting-drop vapour-diffusion method. Protein solution at a concentration of 10 mg  $\text{ml}^{-1}$  was equilibrated against 500  $\mu\text{l}$  reservoir solution in CrysChem plates (Charles Supper Co.) at 293 K. Each droplet was prepared by mixing equal volumes (2  $\mu\text{l}$ ) of protein and reservoir solutions. Crystals were obtained with Crystal Screen and Crystal Screen Lite (Hampton Research) and the chosen crystallization conditions were further optimized using fine intervals of precipitant concentration and pH as well as various combinations of salt additives. For data collection, crystals were transferred stepwise into a crystallization buffer containing a final 25% final concentration of

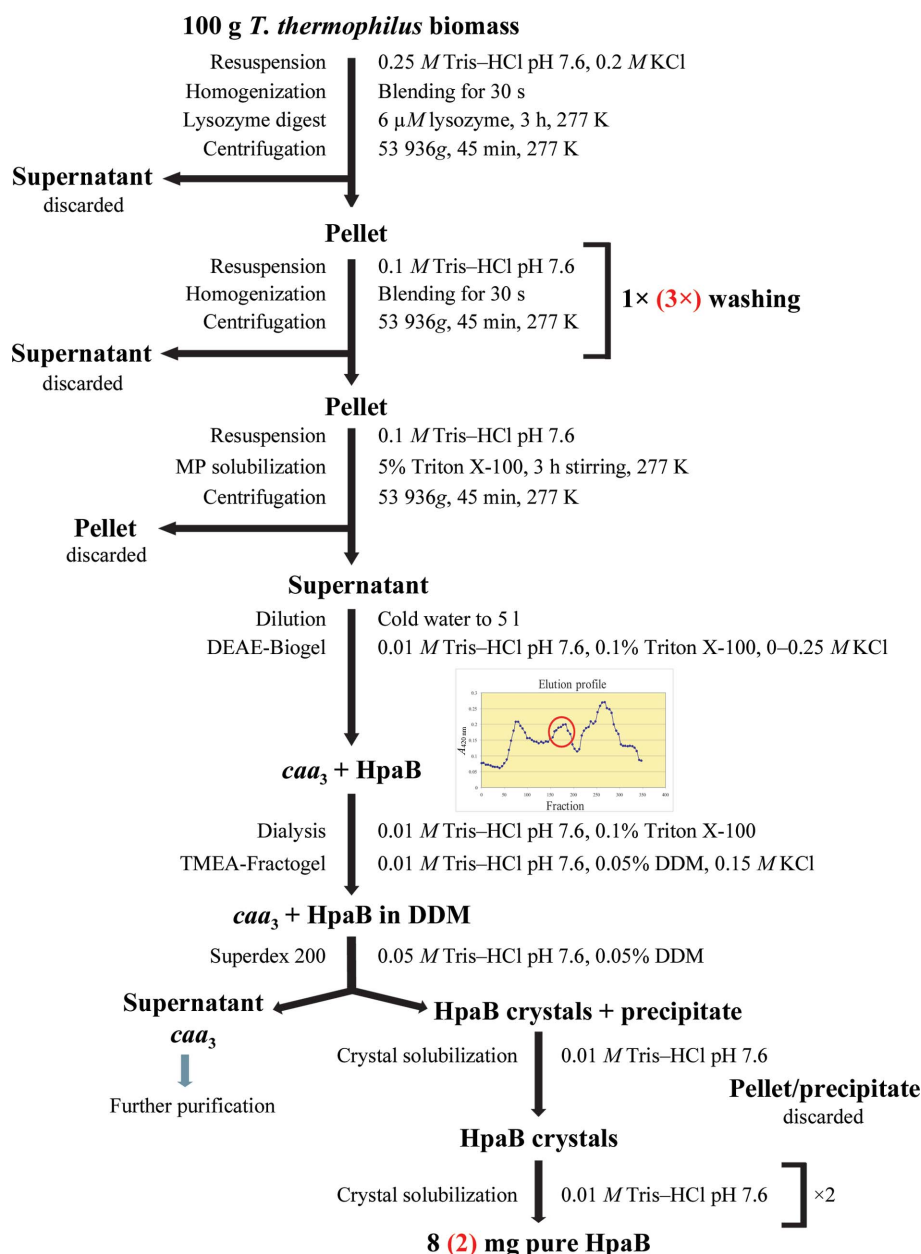


**Figure 2**  
Purification scheme of HpaB.

glycerol as cryoprotectant. High-quality X-ray diffraction data were collected from a single cryocooled crystal measuring  $0.40 \times 0.30 \times 0.30$  mm at liquid-nitrogen temperature (93 K). The intensity data were collected on a Rigaku MicroMax-007MX home-source rotating-anode generator using an R-AXIS<sup>++</sup> detector. The data were processed and scaled using the *HKL-2000* suite of programs (Otwinowski & Minor, 1997) and were further processed using the *CCP4* suite (Collaborative Computational Project, Number 4, 1994).

### 3. Results and discussion

#### 3.1. Isolation, identification and crystallization of native HpaB

During the initial step in the isolation of membrane proteins from *T. thermophilus* HB8 by ion-exchange chromatography on DEAE-Biogel agarose (Soulimane *et al.*, 2002) with subsequent detergent exchange and gel filtration, crystals of an unknown protein spontaneously formed in the elution fraction containing *caa*<sub>3</sub> cytochrome *c* oxidase (Fig. 1*a*). The observed phenomenon was identified to be the result of incomplete removal of soluble proteins during the purification of the respiratory-chain complexes of *T. thermophilus*. As the starting amount of *T. thermophilus* cells was relatively large (100 g), the three washing steps introduced into the purification scheme were not sufficient to remove all of the soluble cytoplasmic proteins. This was demonstrated by the fact that the obtained yields of the protein depended on the amount of cells taken at the beginning of the procedure and also on the number of washes performed during the purification prior to solubilization of membrane proteins. Therefore, production of the protein, further identified as HpaB (see below), could be controlled by the number of washing steps after cell lysis, *i.e.* the greater the number of washing steps, the less crystalline HpaB was generated. This procedure yielded approximately 2 mg purified HpaB after three washing steps and 8 mg protein after one washing step when 100 g biomass was used. Although purification of proteins by crystallization is a known approach among structural biologists, to our knowledge a case such as this, in which a co-purifying protein crystallizes spontaneously during the isolation of an integral membrane protein, has not been described in the literature. Subsequently, the protein could be purified by recrystallization, characterized and used for controlled crystal growth and structure determination.

The protein was further analyzed by mass spectrometry (Aberdeen Proteomics, University of Aberdeen, Scotland). This, together with database mining, led to the identification of the protein as a 481-amino-acid residue oxygenase component of 4-hydroxyphenylacetate 3-monooxygenase (HpaB) with a molecular weight of 54 303 Da and an isoelectric point of 5.96. Additionally, Edman degradation was used to determine the six N-terminal residues, confirming the integrity of the protein.

Crystals of HpaB of approximately 5–10 µm in size formed spontaneously (Fig. 1*a*) from a solution comprising a mixture of detergent, several membrane proteins and a heavy precipitate. Although SDS-PAGE analysis of this mixture shows a smear owing to the presence of residual Triton X-100 and excess lipids in the sample (lane 1 in Fig. 1*b*), the band at around 54 kDa can easily be detected as the major component. Further recrystallization experiments as described in detail in §2 led to highly purified protein as shown on SDS-PAGE (lane 4 in Fig. 1*b*). This sample has been used to grow crystals under controlled conditions using the sitting-drop vapour-diffusion method, generating large and well shaped crystals (Fig. 1*c*).

The elution profile of native HpaB on gel filtration on Superdex 200 shows an elution maximum at a molecular weight of approxi-

**Table 1**

Crystallographic parameters and data-processing statistics for native HpaB from *T. thermophilus*.

Values in parentheses are for the highest resolution shell.

|                                 |                    |
|---------------------------------|--------------------|
| Source/wavelength               | Cu Kα              |
| Resolution (Å)                  | 50–1.82 (1.9–1.82) |
| Space group                     | <i>I</i> 222       |
| Unit-cell parameters (Å)        |                    |
| <i>a</i>                        | 91.3               |
| <i>b</i>                        | 99.8               |
| <i>c</i>                        | 131.7              |
| No. of measurements             | 247085             |
| No. of unique reflections       | 66822              |
| Completeness (%)                | 99.8 (99.5)        |
| Multiplicity                    | 3.8 (2.9)          |
| Average <i>I</i> /σ( <i>I</i> ) | 25.1 (8.8)         |
| <i>R</i> <sub>merge</sub>       | 0.061 (0.38)       |

mately 200 kDa, suggesting the presence of tetrameric HpaB. This fact is supported by the findings of Kim and coworkers, who showed that recombinant HpaB crystallizes as a tetramer (Kim, Hisano *et al.*, 2007; Kim, Miyatake *et al.*, 2007). The elution profile of HpaB superimposes with the elution profile of *caa*<sub>3</sub> cytochrome *c* oxidase and they co-elute with the same elution maximum during size-exclusion chromatography using Superdex 200. Although the molecular weight of *caa*<sub>3</sub> is ~140 kDa owing to the bound detergent (dodecyl-β-D-maltoside), it elutes with an apparent molecular weight of ~200 kDa corresponding to the molecular weight of tetrameric HpaB.

Native HpaB purified by initial crystallization was subsequently concentrated to 10 mg ml<sup>-1</sup> and subjected to screening using Crystal Screen and Crystal Screen Lite (Hampton Research) to identify optimal conditions for crystallogenesis. Owing to the susceptibility of HpaB to crystal formation, microcrystal formation was observed in all precipitating agents in Crystal Screen and Crystal Screen Lite. However, well shaped crystals of HpaB were formed under conditions No. 6 [0.2 M magnesium chloride hexahydrate, 0.1 M Tris-HCl pH 8.5, 15% (w/v) PEG 4000], No. 13 [0.2 M trisodium citrate tribasic dihydrate, 0.1 M Tris-HCl pH 8.5, 15% (v/v) PEG 400], No. 17 [0.2 M lithium sulfate monohydrate, 0.1 M Tris-HCl pH 8.5, 15% (w/v) PEG 4000] and No. 22 [0.2 M sodium acetate trihydrate, 0.1 M Tris-HCl pH 8.5, 15% (w/v) PEG 4000] of Crystal Screen Lite. They appeared within 12 h and reached dimensions of 0.3 × 0.25 × 0.1 mm after 1–2 d. Numerous optimization trials led to the identification of the condition 0.2 M trisodium citrate trihydrate, 0.1 M Tris-HCl pH 8.5, 12% (w/v) PEG 4000, resulting in optically perfect crystals which appeared after 24 h and grew slowly within 7 d to reach dimensions of 0.2 × 0.17 × 0.15 mm (Fig. 1*c*). The obtained crystals were subjected to X-ray investigation after cryocooling in the presence of crystallization solution containing 25% glycerol. Only crystals grown using the optimized condition diffracted to 1.8 Å resolution. Interestingly, despite the use of different crystallization conditions, native HpaB crystallizes in the orthorhombic space group *I*222, similar to its recombinant form as reported previously (Kim, Miyatake *et al.*, 2007), with similar unit-cell parameters *a* = 91.3, *b* = 99.8, *c* = 131.7 Å. Such a phenomenon has also been observed in the case of recombinant HpaB, where two crystallization conditions, 0.4 M 1,6-hexanediol, 0.1 M sodium acetate pH 5.0 and 25% (v/v) glycerol (Kim, Miyatake *et al.*, 2007) and 1.5 M ammonium sulfate, 0.1 M Tris-HCl pH 8.5 and 25% (v/v) glycerol (Kim, Hisano *et al.*, 2007), led to the formation of crystals that belonged to the same space group. From the crystallization results of native HpaB described in this work and those described elsewhere for the recombinant protein (Kim, Hisano *et al.*, 2007; Kim, Miyatake *et al.*, 2007), the nucleation process of HpaB crystals is deduced to initiate spontaneously at low tempera-



ture or by slight contact with any precipitating agent favouring crystals growth in the *I*222 crystal packing.

The crystals of native HpaB contained one subunit of the tetrameric protein in the asymmetric unit. This results in a Matthews coefficient  $V_M$  of  $2.8 \text{ \AA}^3 \text{ Da}^{-1}$  (Matthews, 1968), corresponding to a solvent content of 55.4%. Crystallographic data and data-collection statistics are summarized in Table 1.

Molecular replacement was performed using *MOLREP* (Collaborative Computational Project, Number 4, 1994) with the known recombinant HpaB structure determined by Kim, Hisano *et al.*, 2007 (PDB code 2yyg) as a model; the best solution had an *R* factor of 29.8% and a correction coefficient of 0.816. Refinement of the structure of native HpaB as well as structural comparison of the native and the recombinant proteins is in progress.

This work was supported by the Science Foundation Ireland BICF685 to TS.

## References

- Alfieri, A., Fersini, F., Ruangchan, N., Prongjit, M., Chaiyen, P. & Mattevi, A. (2007). *Proc. Natl Acad. Sci. USA*, **104**, 1177–1182.
- Arias-Barrau, E., Sandoval, A., Naharro, G., Olivera, E. R. & Luengo, J. M. (2005). *J. Biol. Chem.* **280**, 26435–26447.
- Chaiyen, P., Suadee, C. & Wilairat, P. (2001). *Eur. J. Biochem.* **268**, 5550–5561.
- Collaborative Computational Project, Number 4 (1994). *Acta Cryst.* **D50**, 760–763.
- Cooper, R. A. & Skinner, M. A. (1980). *J. Bacteriol.* **143**, 302–306.
- Galan, B., Diaz, E., Prieto, M. A. & Garcia, J. L. (2000). *J. Bacteriol.* **182**, 627–636.
- Galan, B., Kolb, A., Garcia, J. L. & Prieto, M. A. (2001). *J. Biol. Chem.* **276**, 37060–37068.
- Gelder, B. F. van (1966). *Biochim. Biophys. Acta*, **118**, 36–46.
- Gibello, A., Suarez, M., Allende, J. L. & Martin, M. (1997). *Arch. Microbiol.* **167**, 160–166.
- Kadiyala, V. & Spain, J. C. (1998). *Appl. Environ. Microbiol.* **64**, 2479–2484.
- Kim, S.-H., Hisano, T., Takeda, K., Iwasaki, M., Ebihara, A. & Miki, K. (2007). *J. Biol. Chem.* **282**, 33107–33117.
- Kim, S.-H., Miyatake, H., Hisano, T., Iwasaki, W., Ebihara, A. & Miki, K. (2007). *Acta Cryst.* **F63**, 556–559.
- Matthews, B. W. (1968). *J. Mol. Biol.* **33**, 491–497.
- Otwinowski, Z. & Minor, W. (1997). *Methods Enzymol.* **276**, 307–326.
- Prieto, M. A. & Garcia, J. L. (1994). *J. Biol. Chem.* **269**, 22823–22829.
- Smith, P. K., Krohn, R. I., Hermanson, G. T., Mallia, A. K., Gartner, F. H., Provenzano, M. D., Fujimoto, E. K., Goeke, N. M., Olson, B. J. & Klenk, D. C. (1985). *Anal. Biochem.* **150**, 76–85.
- Soulimane, T., Kiefersauer, R. & Than, M. E. (2002). *Membrane Protein Purification and Crystallization*, edited by C. Hunte, G. von Jagow & H. Schagger, pp. 229–251. San Diego: Elsevier.
- Sucharitakul, J., Chaiyen, P., Entsch, B. & Ballou, D. P. (2005). *Biochemistry*, **44**, 10434–10442.
- Sucharitakul, J., Chaiyen, P., Entsch, B. & Ballou, D. P. (2006). *J. Biol. Chem.* **281**, 17044–17053.
- Thotsaporn, K., Sucharitakul, J., Wongratana, J., Suadee, C. & Chaiyen, P. (2004). *Biochim. Biophys. Acta*, **1680**, 60–66.
- Xun, L. & Sandvik, E. R. (2000). *Appl. Environ. Microbiol.* **66**, 481–486.